

SYNTHETIC, SPECTROSCOPIC AND THERMAL ASPECTS OF SOME HETEROCHELATES

C. K. Modi and M. N. Patel*

Department of Chemistry, Sardar Patel University, Vallabh Vidyanagar, Gujarat 388 120, India

The present article describes the synthesis, structural features and thermal studies of heterochelates of the type $[M(SB)(benen)(H_2O)] \cdot nH_2O$ [where $H_2SB=(Z)-2-(2,2,2-trifluoro-1-(5-hydroxy-3-methyl-1-phenyl-1H-pyrazol-4-yl)ethylideneamino)benzoic acid, benen=bis(benzylidene)ethylenediamine and $M=Mn(II), Co(II), Ni(II), Cu(II), Zn(II)$ and $VO(IV)$]. The Schiff base (H_2SB) have been characterized on the basis of elemental analysis, IR, 1H and ^{13}C NMR. The heterochelates have been characterized on the basis of elemental analyses, magnetic measurements, solid state conductivity measurements, IR, reflectance spectra, and thermal studies. The FAB mass spectrum of $[Co(SB)(benen)(H_2O)]$ has been carried out. The kinetic parameters such as order of reaction (n) and the energy of activation (E_a) have been reported using Freeman–Carroll method. The pre-exponential factor (A), the activation entropy ($\Delta S^\#$), the activation enthalpy ($\Delta H^\#$) and the free energy of activation ($\Delta G^\#$) have been calculated.$

Keywords: DSC studies, Freeman–Carroll method, heterochelates, Schiff bases, spectroscopic, TG/DTG studies

Introduction

The thermal analysis techniques were extensively used in studying of the thermal behavior of metal complexes [1–4]. Kinetic studies of thermal decomposition reactions may become useful in calculating the parameters like order of reaction (n), activation energy (E_a), entropy change ($\Delta S^\#$), enthalpy change ($\Delta H^\#$), free energy change ($\Delta G^\#$) and pre-exponential factor (A). Thermogravimetry is a process in which a substance is decomposed in the presence of heat, which causes bonds the molecules to be broken [5, 6]. In continuation of our earlier work [7] herein we describe synthetic, thermal and spectroscopic aspects of heterochelates. The suggested structure of the Schiff base (H_2SB) is shown in Scheme 1.

Experimental

Materials

Reagent and solvents

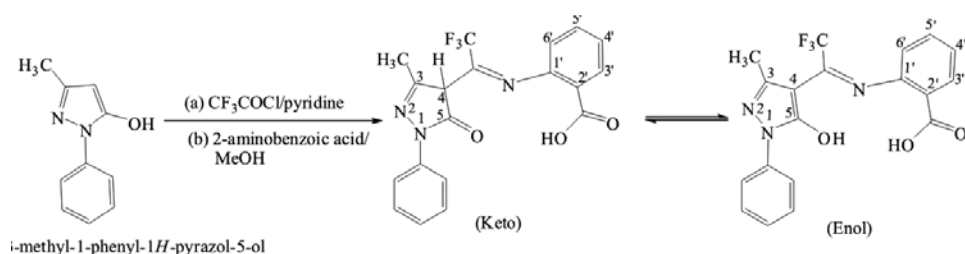
All used chemicals were of analytical grade (E. Merck, or Lancaster) and used without further purification. The organic solvents were purified by standard methods [8].

Synthesis of ligand 3-methyl-1-phenyl-4-trifluoroacetyl-1H-pyrazol-5-one

The ligand 3-methyl-1-phenyl-4-trifluoroacetyl-1H-pyrazol-5-one was synthesized by using trifluoroacetic anhydride in pyridine, following a procedure that reported by Okafor earlier [9]. Yield: 74%; *m.p.* 144°C. 1H NMR (400 MHz, $CDCl_3$): δ (ppm)=2.47 (3H, s, $-CH_3$), [7.45 (1H, t), 7.58 (2H, t), 7.62 (1H, d) aromatic protons], 12.20 (1H, s, $-OH$). Anal. Calc. for $C_{12}H_9N_2O_2F_3$: C, 53.34; H, 3.35; N, 10.49. Found: C, 53.27; H, 3.36; N, 10.49%.

Synthesis of (Z)-2-(2,2,2-trifluoro-1-(5-hydroxy-3-methyl-1-phenyl-1H-pyrazol-4-yl)ethylideneamino)benzoic acid (H_2SB)

An ethanolic solution (50 mL) of 3-methyl-1-phenyl-4-trifluoroacetyl-1H-pyrazol-5-one (10 mmol, 2.70 g) was added to an ethanolic solution (25 mL) of 2-amino benzoic acid (10 mmol, 1.37 g) in a 250 mL of round bottom flask. The mixture was boiled with stirring at reflux temperature for 6 h. The resulting solution was cooled overnight at room temperature in an evaporating dish. The solvent was



Scheme 1 Synthesis and structure of the Schiff base ligand (H_2SB)

* Author for correspondence: jeenenpatel@yahoo.co.in

removed after evaporation and brown oily product was obtained, washed with diethyl ether (30 mL). After filtration, the light brown powdered was dried in vacuo to constant mass and finally purified by recrystallizing in absolute ethanol. Yield: 3.09 g (76%); *m.p.*: 64°C. FTIR (KBr, cm⁻¹): 2815 (-CH₃), 1693 (C=O), 1635 (C=N), 1591.2 (COO⁻, asymmetric), 1392.5 (COO⁻, symmetric). ¹H NMR (400 MHz, CDCl₃): δ (ppm)=2.19 (3H, s, -CH₃); 11.72 (1H, s, 5-OH); [7.29 (1H, t), 7.38 (2H, t), 7.95 (2H, d) for aromatic protons]; 7.65 (1H, t, C3'-H), 7.49 (1H, t, C4'-H), 7.42 (1H, t, C5'-H), 7.85 (1H, d, C6'-H). ¹³C NMR (400 MHz, CDCl₃): δ (ppm)=16.99 (CH₃), 109.73 (C1), 156.64 (C2), 161.2 (C5), [116.13, 116.43, 119.0, 137.96 for aromatic ring], 151.09 (C1'), 116.43 (C2'), 132.11 (C3'), 125.18 (C4'), 135.0 (C5'), 128.86 (C6'), 170.85 (C2'CO), CF₃ [10] and C=N not observed. Anal. Calc. for C₁₉H₁₄N₃O₃F₃: C, 58.65; H, 3.62; N, 10.79. Found: C, 58.63; H, 3.63; N, 10.81%.

Synthesis of bis(benzylidene)ethylenediamine (benen)

The ligand (benen) was synthesized according to the procedure described in the literature [11].

Synthesis of heterochelates

The preparation of heterochelates were carried out by mixing hot methanolic solution (50 mL) of metal nitrate (10 mmol) or an aqueous solution (50 mL) of VOSO₄·5H₂O (10 mmol, 2.53 g) and a hot methanolic solution (50 mL) of the Schiff base (H₂SB) (10 mmol, 3.89 g) and bis(benzylidene)ethylenediamine (10 mmol, 2.36 g). The heterochelates were formed by heating the mixture in a water bath for 2 h at 60°C. The mixture was kept overnight at room temperature. The obtained colored crystals were collected by filtration, washed with water, methanol and finally with diethyl ether and dried in air.

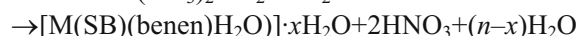
Methods

The metal content of the heterochelates were analyzed by the EDTA titration technique [12]. A 100 mg sample of the VO(IV) compound was placed in a silica crucible, decomposed by gentle heating and then treated with 1–2 mL of concentrated HNO₃, 2–3 times. Orange colored residues (V₂O₅) were obtained after decomposition and complete drying [13]. Carbon, hydrogen and nitrogen were analyzed with the Perkin Elmer, USA 2400-II CHN analyzer. The magnetic moments were obtained by the Gouy's method using mercury tetrathiocyanato cobaltate(II) as a calibrant ($\chi_g=16.44 \cdot 10^{-6}$ c.g.s. units at 20°C). Diamagnetic corrections were made using Pascal's constant. A simultaneous TG/DTG had been obtained by a model

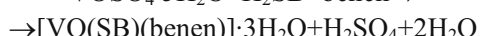
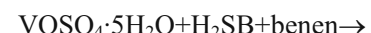
Pyris-1 TGA, Perkin Elmer, USA. The experiments were performed in N₂ atmosphere at a heating rate of 10°C min⁻¹ in the temperature range 50–1000°C, using Al₂O₃ crucible. The sample sizes are ranged in mass from 2.5–6 mg. The DSC was recorded using DSC 2920, TA Instrument, USA. The DSC curves were obtained at a heating rate of 10°C min⁻¹ in N₂ atmosphere over the temperature range of 50–400°C, using aluminum crucible. The IR spectra were recorded on a FTIR Nicolet-400D spectrophotometer using KBr pellets. NMR spectra were recorded on a model Avance 400 Bruker FT-NMR instrument and CDCl₃ used as a solvent. The FAB mass spectrum of the heterochelate was recorded at SAIF, CDRI, Lucknow with JEOL SX-102/DA-6000 mass spectrometer. The reflectance spectra of the complexes were recorded in the range of 1700–350 nm (as MgO discs) on a Beckman DK-2A spectrophotometer.

Results and discussion

The analytical and physical data of the ligand and its heterochelates are presented in Table 1. The heterochelates are colored and stable in air. They are insoluble in water, alcohol and DMF but soluble in DMSO. All the heterochelates are non electrolyte in nature. The formations of the heterochelates are assumed according to the following balanced chemical Eq. (1).



where M=Mn(II), Co(II) and Cu(II) x=0, Zn(II) x=0.5 and Ni(II) x=1.



Spectroscopic characterization of heterochelates

Infrared Spectra

The important infrared spectral bands and their tentative assignments for the synthesized heterochelates were recorded as KBr disks and are summarized in Table 2.

In the investigated heterochelates, the bands observed in the region 3400–3450, 1295–1300, 860–870 and 715–717 cm⁻¹ are attributed to –OH stretching, bending, rocking and wagging vibrations, respectively due to the presence of water molecules [14]. The presence of later band indicates the coordination nature of the water molecule [15]. The later band was not observed in the spectra of oxovanadium(IV) heterochelate, indicating the absence of coordinated water molecule. The oxovanadium(IV) heterochelate exhibits a strong absorption band near ~958 cm⁻¹, which

Table 1 Analytical and physical data of ligands and its heterochelates

Compound	Colour (M.Wt./g mol ⁻¹)	Found (calcd.)/%				$\mu_{\text{eff}}/\text{B.M.}$	Yield/%
		C	H	N	M		
Ligand (H ₂ SB)	Light brown (389.10)	58.63 (58.65)	3.63 (3.62)	10.81 (10.79)	—	—	76
Ligand (benen)	Orange yellow (236.13)	81.34 (81.38)	6.85 (6.82)	11.87 (11.85)	—	—	70
[Mn(SB)(benen)(H ₂ O)]	Light cream (696.16)	60.39 (60.38)	4.36 (4.34)	10.09 (10.06)	7.92 (7.89)	6.02	66
[Co(SB)(benen)(H ₂ O)]	Light brown (700.16)	59.99 (60.04)	4.32 (4.31)	10.04 (10.00)	8.44 (8.41)	4.06	66
[Ni(SB)(benen)(H ₂ O)]·H ₂ O	Light green (717.17)	58.70 (58.61)	4.51 (4.48)	9.78 (9.76)	8.19 (8.18)	2.84	74
[Cu(SB)(benen)(H ₂ O)]	Light bluish (704.15)	59.69 (59.70)	4.30 (4.28)	9.97 (9.94)	9.05 (9.02)	1.78	72
[Zn(SB)(benen)(H ₂ O)]·1/2H ₂ O	Light cream (714.15)	58.89 (58.86)	4.37 (4.36)	9.79 (9.80)	9.17 (9.15)	Diamag.	68
[VO(SB)(benen)]·3H ₂ O	Dark green (744.18)	56.52 (56.48)	4.67 (4.60)	9.42 (9.41)	6.87 (6.84)	1.80	70

Table 2 The characteristic IR bands of ligands and its heterochelates in cm⁻¹

Compounds	V _(-OH)	V _(C=N)	V _(C-O)	V _(COO⁻)			V _(M-N)	V _{(M-O)^[a]}	V _{(M-O)^[b]}
				Antisymmetric	Symmetric	Δv			
Ligand (H ₂ SB)	—	1635	—	1591.4	1392.5	198.2	—	—	—
Ligand (benen)	—	1626	—	—	—	—	—	—	—
[Mn(SB)(benen)(H ₂ O)]	3430	1614	1323	1589.2	1384.4	204.8	516	476	423
[Co(SB)(benen)(H ₂ O)]	3446	1616	1323	1591.2	1384.4	205.2	518	480	425
[Ni(SB)(benen)(H ₂ O)]·H ₂ O	3460	1612	1325	1593.3	1384.4	208.5	518	483	420
[Cu(SB)(benen)(H ₂ O)]	3442	1602	1324	1586.2	1384.4	202.1	518	472	423
[Zn(SB)(benen)(H ₂ O)]·1/2H ₂ O	3429	1614	1326	1593.1	1384.4	206.2	515	480	422
[VO(SB)(benen)]·3H ₂ O	3520	1620	1323	1592.4	1384.4	205.7	515	472	420

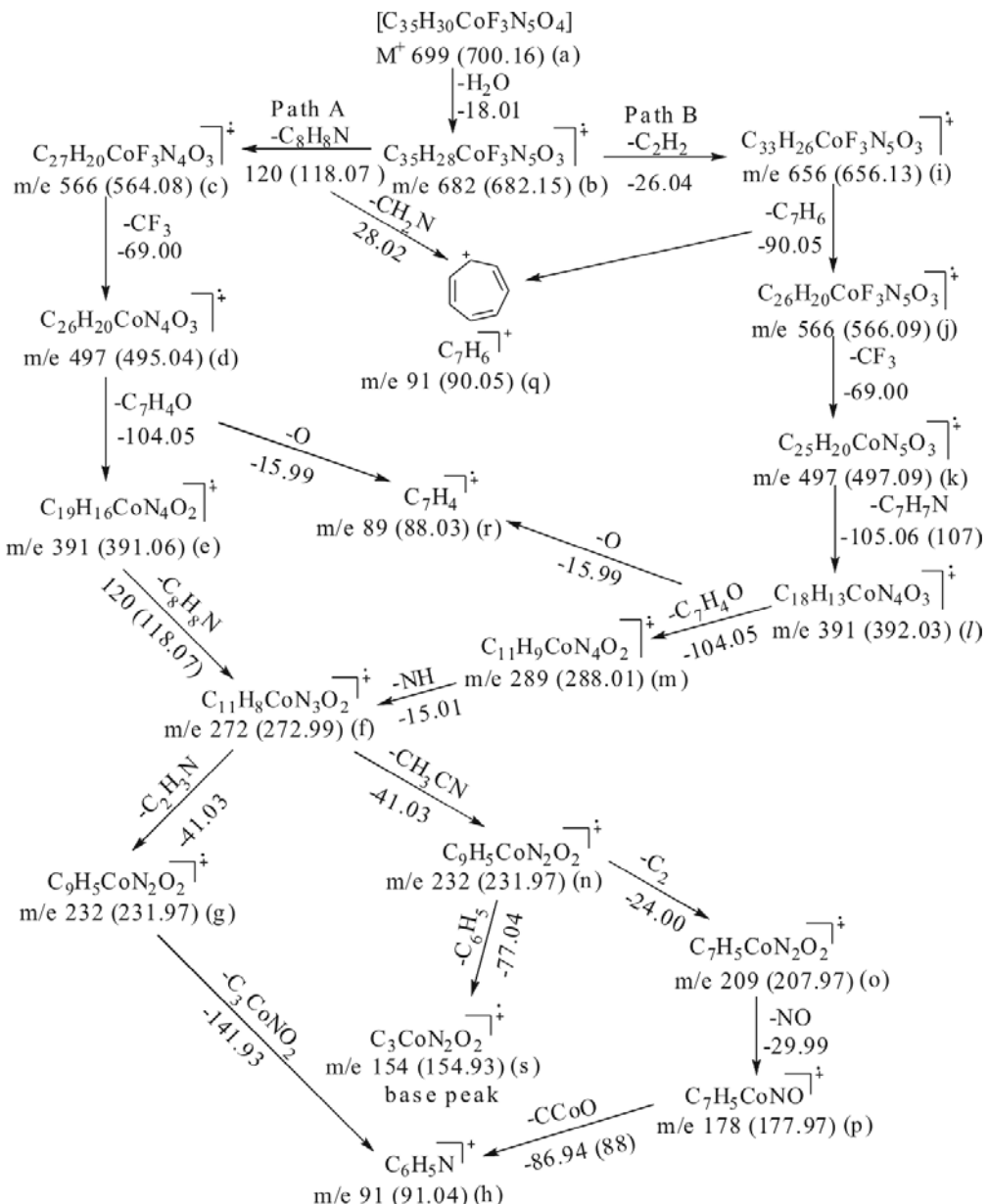
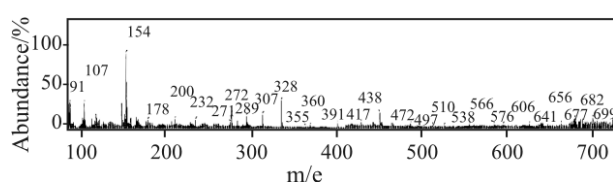
[a]pyrazolone, [b]carboxyl

has been assigned to $\nu_{\text{V=O}}$ band [16]. The $\nu_{\text{as(COO}^-)}$ and $\nu_{\text{s(COO}^-)}$ vibrational frequencies, together with the $\Delta\nu_{\text{(COO}^-)}$ values for the carboxylate group of the Schiff base (H₂SB) and their heterochelates are listed in Table 2. All of the heterochelates produced a $\Delta\nu_{\text{COO}^-}$ value of $>200 \text{ cm}^{-1}$, suggesting unidentate carboxylate coordination to the central metal ions [17, 18]. The strong band at 1635 cm⁻¹ attributable to the C=N stretching vibration of the Schiff base ligand is shifted to a region of 1602–1620 cm⁻¹ in the heterochelates, indicating the coordination of the azomethine nitrogen [19]. The band at 1693 cm⁻¹ for $\nu_{(\text{C}^{\text{s}}=\text{O})}$ (see Scheme 1) in the free ligand (H₂SB) is absent in the heterochelates and new absorption bands attributed to $\nu_{(\text{C}-\text{O})}$ [20] are observed at 1323–1326 cm⁻¹, which indicates that the pyrazolone undergoes isomerization from the keto form to the enol form during the reaction and then coor-

dinates through a deprotonated oxygen. In the far-IR region, three new bands at 515–518, 472–483 and 420–425 cm⁻¹ in the heterochelates are assigned to $\nu_{(\text{M}-\text{N})}$ [21], $\nu_{(\text{M}-\text{O})}$ pyrazolone and $\nu_{(\text{M}-\text{O})}$ carboxyl [22] groups, respectively. All of these data confirm the fact that H₂SB behaves as a dinegative tridentate ligand forming a conjugated chelate ring, with the ligand existing in the heterochelates in the enolized form.

Mass spectral studies

The recorded mass spectra (Fig. 1) and the molecular ion peak for the heterochelate [Co(SB)(benen)(H₂O)] have been used to confirm the molecular formulae. The fragmentation pattern is given in Scheme 2. The first peak at *m/e* 699 represents the molecular ion peak of the complex with 12.85% abundance.

**Scheme 2** The suggested fragmentation pattern of $[\text{Co}(\text{SB})(\text{benen})(\text{H}_2\text{O})]^+$ **Fig. 1** The mass spectrum of $[\text{Co}(\text{SB})(\text{benen})(\text{H}_2\text{O})]$

The primary fragmentation of the heterochelate takes place due to the loss of one coordinated water molecule followed by two possible pathways for the fragmentation of the heterochelate. Scheme 2 demonstrates the two possible degradation pathways for the investigated heterochelate. In path (A), loss of $\text{C}_8\text{H}_8\text{N}$

group from the species (b) to give species (c) with peak at m/e 566 (5.51%). The $\text{C}_8\text{H}_8\text{N}$ group further degrades with the loss of CH_2N to give a peak at m/e 91 with 34.28% abundance represents the stable species C_7H_6 ion. The species (c) further degrades with the subsequent loss of CF_3 , $\text{C}_7\text{H}_4\text{O}$ and $\text{C}_8\text{H}_8\text{N}$ forming species (d), (e) and (f) with their peaks at m/e 497 (4.13%), 391 (8.27%) and 272 (19.31%), respectively. In path (B), the radical C_2H_2 may be lost in the beginning to give peak at m/e 656 (13.79%) due to formation of $[\text{C}_{33}\text{H}_{26}\text{CoF}_3\text{N}_5\text{O}_4]^+$ ion. Subsequent loss of C_7H_6 , CF_3 , $\text{C}_7\text{H}_7\text{N}$, $\text{C}_7\text{H}_4\text{O}$ and NH groups from the species (i) giving peaks at m/e 566 (4.82%), 497 (4.13%), 391 (8.27%), 289 (16.55%) and 272 (20.68%) due to the formation of species (j), (k),

Table 3 Electronic parameters of the Co(II) and Ni(II) heterochelates[a]

Heterochelates	Observed bands/cm ⁻¹			v ₂ /v ₁	B	β	β ₀	10 Dq
	v ₁	v ₂	v ₃					
[Co(SB)(benen)(H ₂ O)]	9300	18050	18900	1.94	714	0.73	26.5	10415
[Ni(SB)(benen)(H ₂ O)]·H ₂ O	10200	17650	23800	1.73	723	0.70	29.7	10200

[a] The ligand field splitting energy (10 Dq), interelectronic repulsion parameter (B) and covalency factor (nephelauxetic ratio) for the Co(II) and Ni(II) complexes were calculated using the secular equations given by E. König [31]:

For Co(II) complex

$$10 \text{ Dq} = 1/2 [(2v_1 - v_3) + (v_3^2 + v_1 v_3 - v_1^2)^{1/2}]$$

$$15B = v_3 - 2 v_1 + 10 \text{ Dq}$$

$$\beta = B/B_0 \quad [B_0 \text{ (free ion)} = 971]$$

$$\beta_0 = (1 - \beta) \cdot 100$$

For Ni(II) complex

$$10 \text{ Dq} = v_1$$

$$15B = (v_2 + v_3) - 3 v_1$$

$$\beta = B/B_0 \quad [B_0 \text{ (free ion)} = 1030]$$

$$\beta_0 = (1 - \beta) \cdot 100$$

(l), (m) and (f), respectively. The sharp peak (base peak) observed at *m/e* 154 represents the stable species C₃CoN₂O₂ with 99.6% abundance.

Magnetic moments and electronic spectra

In order to shed some light on the geometrical structure of the heterochelates, the reflectance spectra of the heterochelates were recorded in the solid phase at room temperature. The reflectance spectra of the Mn(II) heterochelate shows absorption bands at ~14600, ~19720 and ~24400 cm⁻¹ assignable to ⁶A_{1g}→⁴T_{1g}, ⁶A_{1g}→⁴T_{2g} and ⁶A_{1g}→⁴A_{1g}, ⁴E_g transitions, respectively, in an octahedral environment around the Mn(II) ion. The magnetic moment value of the Mn(II) heterochelate is 6.02 B.M. due to a high-spin d⁵-system with an octahedral geometry [23]. For the Co(II) heterochelate, the reflectance spectra exhibits the bands of medium intensity at ~9300, ~18050 and ~18900 cm⁻¹, which may reasonably be assigned to ⁴T_{1g}(F)→⁴T_{2g}(F), ⁴T_{1g}(F)→⁴A_{2g}(F) and ⁴T_{1g}(F)→⁴T_{1g}(P) transitions, respectively, of an octahedral geometry around the metal ion [24] and the magnetic moment value is observed to be of 4.06 B.M. The electronic spectra of the Ni(II) heterochelate exhibits absorption bands at ~10200, ~17650 and ~23800 cm⁻¹ assignable to ³A_{2g}(F)→³T_{2g}(F), ³A_{2g}(F)→³T_{1g}(F) and ³A_{2g}(F)→³T_{1g}(P) transitions respectively, in an octahedral geometry. The value of the magnetic moment (2.84 B.M.) may be taken as additional evidence for their octahedral structure [25–28]. The Cu(II) heterochelate display a broad band at ~15440 cm⁻¹ due to the ²E_g→²T_{2g} transition and the magnetic moment value is 1.78 B.M., which is close to spin-only value (1.73 B.M.) expected for an unpaired electron, which offers the possibility of an octahedral geometry [29]. The oxovanadium(IV) heterochelate exhibits three spin-allowed transitions in the ~13200, ~15800 and ~23900 cm⁻¹ regions, which have been assigned to ²B₂→²E (v₁), ²B₂→²B₁ (v₂) and ²B₂→²A₁ (v₃) transitions, respectively [30]. The oxovanadium(IV) heterochelate exhibits magnetic moment corresponding to the

spin-only value of 1.80 B.M. The Zn(II) heterochelate is diamagnetic as expected for d¹⁰ system. The values of the electronic parameters [31], such as the ligand field splitting energy (10 Dq), Racah interelectronic repulsion parameter (B), nephelauxetic ratio (β) and ratio v₂/v₁ are summarized in Table 3.

Thermodynamic studies

The thermodynamic activation parameters of the decomposition process of the heterochelates such as energy of activation (*E*_a) and order of reaction (*n*) were evaluated graphically by employing the Freeman–Carroll method [32] using the following relation:

$$[(-E_a/2.303R)\Delta(1/T)]/\Delta\log w_r = -n + \Delta\log(dw/dt)/\Delta\log w_r \quad (1)$$

where *T* is the temperature in K, *R* is gas constant, *w_r*=*w_c*−*w*; *w_c* is the mass loss at the completion of the reaction and *w* is the total mass loss up to time *t*. *E*_a and *n* are the energy of activation and order of reaction, respectively. A typical curve of [Δlog(dw/dt)/Δlogw_r] vs. [Δ(1/T)/Δlogw_r] for the Ni(II) heterochelate is shown in Fig. 2. The slope of the plot gave the value of *E*_a/2.303*R* and the order of reaction (*n*) was determined from the intercept.

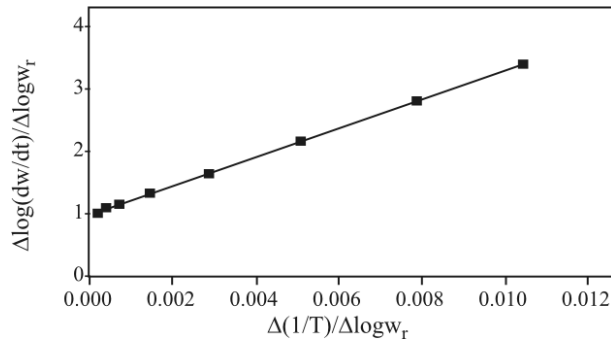


Fig. 2 Freeman-Carroll plot for thermal degradation of [Ni(SB)(benen)H₂O]·H₂O

The thermal behavior of the prepared heterochelates

The thermal behaviour of the synthesized heterochelates has been characterized on the basis of TG/DTG and DSC methods. Thermoanalytical data of the heterochelates are given in Table 4.

The TG/DTG and DSC curves of the heterochelate $[\text{Ni}(\text{SB})(\text{benen})(\text{H}_2\text{O})]\cdot\text{H}_2\text{O}$ represented in Figs 3

and 4, respectively. The decomposition of the heterochelate undergoes in four stages. The first endothermic peak in DSC at 108°C, in the temperature range 50–130°C, with the mass loss (obs. 2.56%; calcd. 2.51%) corresponds to the loss of one mole of lattice water molecule [33]. The loss of one mole of lattice water molecule is of first order reaction and the value of the energy of activation [32] for the

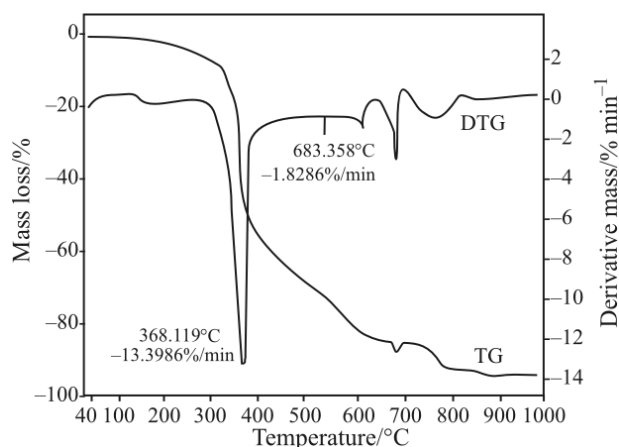


Fig. 3 TG/DTG curves of $[\text{Ni}(\text{SB})(\text{benen})(\text{H}_2\text{O})]\cdot\text{H}_2\text{O}$

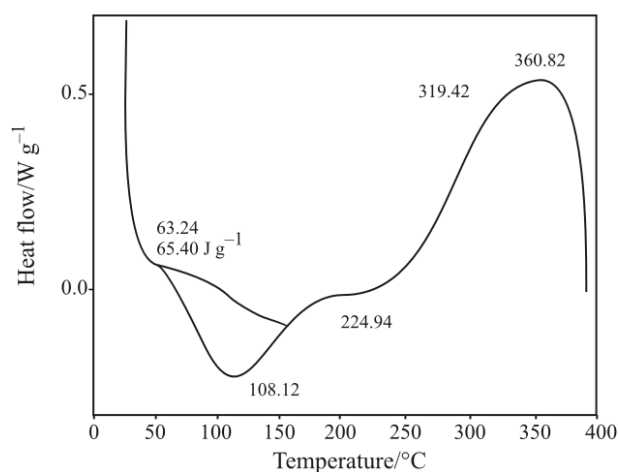


Fig. 4 DSC curves of $[\text{Ni}(\text{SB})(\text{benen})(\text{H}_2\text{O})]\cdot\text{H}_2\text{O}$

Table 4 Thermoanalytical results (TG, DTG and DSC) of heterochelates

Heterochelates	TG range/°C	DTG _{max} /°C	DSC _{max} /°C	Mass loss/% obs. (calc.)	Assignment
$[\text{Mn}(\text{SB})(\text{benen})(\text{H}_2\text{O})]$	130–260	220	226 (+)	2.65 (2.59)	Loss of one coordinated water molecule
	260–400	329	376 (–)	33.86 (33.92)	Removal of ligand (benen)
	400–850	417	—	52.08 (52.16)	Removal of (SB) ligand molecule
		701	—	88.59* (88.66)	Leaving Mn_2O_3 residue
$[\text{Co}(\text{SB})(\text{benen})(\text{H}_2\text{O})]$	130–240	201	224 (+)	2.71 (2.57)	Loss of one coordinated water molecule
	240–370	347	347 (–)	33.76 (33.72)	Removal of ligand (benen)
	370–850	503	—	52.08 (51.86)	Removal of (SB) ligand molecule
		—	—	88.41* (88.15)	Leaving Co_2O_3 residue
$[\text{Ni}(\text{SB})(\text{benen})(\text{H}_2\text{O})]\cdot\text{H}_2\text{O}$	50–130	—	108 (+)	2.56 (2.51)	Loss of one lattice water molecule
	130–270	202	224 (+)	2.74 (2.51)	Loss of one coordinated water molecule
	270–380	368	—	32.66 (32.92)	Removal of ligand (benen)
	380–930	683	—	54.33 (54.25)	Removal of (SB) ligand molecule
		—	—	92.29* (92.19)	Leaving free Ni residue
$[\text{Cu}(\text{SB})(\text{benen})(\text{H}_2\text{O})]$	100–180	152	—	2.69 (2.55)	Loss of one coordinated water molecule
	180–250	229	250 (+)	33.63 (33.51)	Removal of ligand (benen)
	250–730	289	274 (+)	52.37 (52.67)	Removal of (SB) ligand molecule
		323 (+)	—	88.69* (88.73)	Leaving CuO residue
$[\text{Zn}(\text{SB})(\text{benen})(\text{H}_2\text{O})]\cdot 1/2\text{H}_2\text{O}$	50–140	98	—	1.33 (1.26)	Loss of half mole of lattice water molecule
	140–250	210	228 (+)	2.64 (2.52)	Loss of one coordinated water molecule
	250–360	329	353 (+)	32.69 (32.99)	Removal of ligand (benen)
	360–790	658	—	51.93 (51.86)	Removal of (SB) ligand molecule
		—	—	88.59* (88.63)	Leaving ZnO residue
$[\text{VO}(\text{SB})(\text{benen})]\cdot 3\text{H}_2\text{O}$	50–140	95	102 (+)	7.30 (7.26)	Loss of three lattice water molecules
	140–380	290	296 (+)	31.85 (31.73)	Removal of ligand (benen)
	380–850	417	—	48.57 (48.79)	Removal of (SB) ligand molecule
		—	—	87.72* (87.78)	Leaving V_2O_5 residue

(+): endothermic; (–): exothermic; * Total mass loss

dehydration process is found to be 3.19 kJ mol^{-1} . The second stage between 130 to 270°C with DTG peak at 202°C [33–36], corresponds to the decomposition of one coordinated water molecule. The observed mass loss is 2.74% which is consistent with the theoretical value of 2.51%. This process is accompanied by an endothermic peak at 224°C in DSC curve [33]. Degradation of ligand (benen) takes place in third stage between 270 to 380°C with a mass loss of 32.66% (calcd. 32.92%). The maximum rate of mass loss is indicated by the DTG peak at 368°C. The degradation of benen molecule is a first order reaction with the energy of activation for this stage is $20.54 \text{ kJ mol}^{-1}$. The fourth stage occurs between 380 to 930°C, corresponding to the decomposition of SB ligand molecule, with the mass loss of 54.33% (calcd. 54.25%). The maximum rate of mass loss is indicated by the DTG peak at 683°C. The removal of the Schiff base (SB) is also a first order reaction with the value of the energy of activation is found to be $52.05 \text{ kJ mol}^{-1}$. The total mass loss (92.29%) coincides with the theoretical value of 92.19% (Table 4). The final residue, estimated as free Ni [37, 38], has the observed mass 7.67% as against the calculated value of 8.18%.

The thermal decomposition of the heterochelate $[\text{Mn}(\text{SB})(\text{benen})(\text{H}_2\text{O})]$ undergoes in three stages. The first stage is related to the liberation of one coordinated water molecule from the heterochelate in the temperature range of 130–260°C, accompanied by a mass loss of 2.65% (calcd. 2.59%). The DTG peak corresponding to this stage is found at 220°C. The loss of one coordinated water molecule is a first order reaction and the value of the activation energy for the dehydration process is 4.21 kJ mol^{-1} . In the second stage between 260 to 400°C, the ligand (benen) degrades as one maximum in the DTG curve at 329°C with a mass loss 33.86% (calcd. 33.92%). It is accompanied by an exothermic process at 376°C in the DSC curve. The degradation of benen is of first order and the energy of activation is found to be $16.48 \text{ kJ mol}^{-1}$. The third stage, which occurs in the temperature range 400–760°C with two DTG peaks are observed at 417 and 701°C, corresponding to the decomposition of SB ligand molecule. The observed mass loss (52.08%) is coinciding with the calculated value of 52.16%. The overall mass losses are observed to be 88.59%, which is in well agreement with the calculated value of 88.66%. The final residue, estimated as Mn_2O_3 , has the observed mass 11.36% as against the calculated value of 11.33%.

The heterochelate of $[\text{Co}(\text{SB})(\text{benen})(\text{H}_2\text{O})]$ gives a three-stage decomposition process. The first stage occurs in the temperature range 130–240°C, with the mass loss (2.71%) is due to the removal of one coordi-

nated water molecule from the heterochelate (calcd. 2.57%). The DTG and DSC peaks corresponding to this stage are found at 202 and 224°C, respectively. The second (from 240–370°C) and third (from 370–850°C) stages may be due to the degradation of benen and SB ligand moieties takes place. The observed mass losses in these temperature ranges are 33.76 and 52.08%, respectively. The degradation of the benen and SB are of first order reactions and the energy of activations is found to be 17.37 and $27.38 \text{ kJ mol}^{-1}$, respectively. The overall mass loss 88.41% is as against the theoretical value of 88.15%. The end product estimated as Co_2O_3 , has the observed mass of 11.56% compared with the calculated value of 11.84%.

The thermal decomposition of the heterochelate $[\text{Cu}(\text{SB})(\text{benen})(\text{H}_2\text{O})]$ undergoes in three stages. Degradation of one coordinated water molecule takes place in the first stage between 100 and 180°C with a mass loss of 2.69% (calcd. 2.55%). The maximum rate of mass loss is indicated by the DTG peak at 152°C. This step is of first order reaction and the energy of activation is 3.71 kJ mol^{-1} . The second stage between 180 and 250°C with the DTG peak at 229°C, with the mass loss of 33.63% (calcd. 33.51%) corresponds to the loss of ligand (benen). The removal of benen is of first order reaction and the value of the energy of activation is found to be $13.64 \text{ kJ mol}^{-1}$. The third stage, which occurs in the temperature range 250–730°C with a DTG peak at 289°C, corresponding to the decomposition of SB ligand molecule, the observed mass loss (52.37%), which is coincides with the theoretical value (52.67%). This process is accompanied by two endothermic effects at 274 and 323°C in the DSC curve. The overall mass losses are observed to be 88.69%, which is in good agreement with the calculated value of 88.73%. The final residue, estimated as copper oxide, has the observed mass 11.26% as against the calculated value of 11.29%.

The decomposition of the heterochelate $[\text{VO}(\text{SB})(\text{benen})] \cdot 3\text{H}_2\text{O}$ undergoes in three stages. The thermal dehydration of this heterochelate takes place between 50 to 140°C, with a mass loss of 7.30% (calc. 7.26%). The endothermic peak corresponding to this stage is given by the DSC curve at 102°C. Three moles of lattice water molecules are removed in this stage of dehydration. The loss of three lattice water molecules is of first order reaction and the value of the energy of activation for the dehydration process is 4.14 kJ mol^{-1} . Degradation of ligand (benen) was followed in the second stage between 140 to 380°C with a mass loss of 31.85% (calcd. 31.73%). The maximum rate of mass loss is indicated by the DTG peak at 290°C. The third stage between 380 to 850°C with a DTG peak at 417°C corresponds to the decomposition of the remaining SB ligand molecule.

Table 5 Thermodynamic data of the thermal decomposition of heterochelates

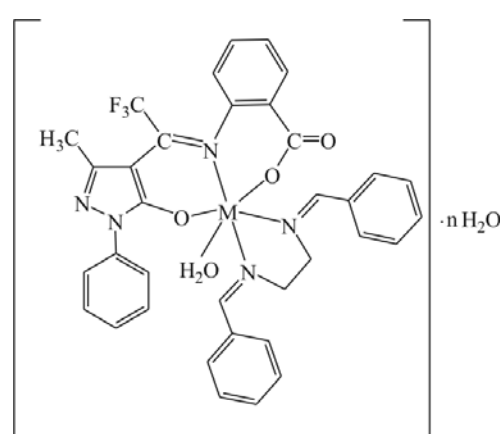
Heterochelates	TG range/°C	$E_a/\text{kJ mol}^{-1}$	n	A/s ⁻¹	$\Delta S^\#/\text{J K}^{-1}\text{mol}^{-1}$	$\Delta H^\#/\text{kJ mol}^{-1}$	$\Delta G^\#/\text{kJ mol}^{-1}$
[Mn(SB)(benen)(H ₂ O)]	130–260	4.20	1.00	0.06	-102.99	0.11	50.88
	260–400	16.48	1.00	1.46	-98.78	1.47	70.97
	400–850	31.87	1.00	21.00	-96.89	26.13	93.01
[Co(SB)(benen)(H ₂ O)]	130–240	4.21	1.00	0.08	-102.68	0.44	46.95
	240–370	17.37	1.00	1.58	-98.69	12.22	73.38
	370–850	27.38	1.00	3.80	-97.86	20.93	96.85
[Ni(SB)(benen)(H ₂ O)]·H ₂ O	50–130	3.19	0.95	0.08	-102.99	0.08	38.70
	130–270	4.32	1.10	0.06	-102.85	0.26	50.45
	270–380	20.54	1.00	2.80	-98.21	15.21	78.18
	380–930	52.05	1.00	37.00	-96.42	42.33	134.5
[Cu(SB)(benen)(H ₂ O)]	100–180	3.71	1.05	0.07	-102.91	0.17	43.91
	180–250	13.64	1.00	1.71	-98.80	9.46	59.08
	250–730	24.73	1.00	24.00	-96.93	20.26	72.79
[Zn(SB)(benen)(H ₂ O)]·1/2H ₂ O	50–140	3.26	0.96	0.08	-102.87	0.18	38.34
	140–250	4.25	1.12	0.06	-102.87	0.24	49.92
	250–360	16.59	1.00	1.58	-98.73	11.50	70.05
	360–790	23.51	1.00	0.67	-99.08	15.75	108.19
[VO(SB)(benen)]·3H ₂ O	50–140	4.14	0.97	0.13	-102.11	0.98	39.88
	140–380	17.34	1.00	1.01	-98.97	11.78	78.00
	380–850	31.86	1.00	25.90	-98.00	24.06	115.98

The observed mass loss is 48.57%, which is consistent with the theoretical value of 48.79%. The end product, estimated as V₂O₅, has the observed mass of 12.27% compared with the calculated value of 12.22%.

The TG curve of [Zn(SB)(benen)(H₂O)]·1/2H₂O is characterized by four degradation steps in the range 50–140, 140–250, 250–360 and 360–790°C. Elimination of half mole of lattice water molecule (calcd. 1.26%; obs. 1.33%) is the first step. The second step consumed one coordinated water molecule (calcd. 2.52%, obs. 2.64%). The first and second dehydration steps are of first order reaction and the values of the energy of activation are found to be 3.27 and 4.25 kJ mol⁻¹, respectively. The ligand (benen) is assumed to be evolved in the third step (calcd. 32.99%; obs. 32.69%). Moreover, the fourth step in the curve shows removal of SB ligand molecule up to 790°C after which a constant mass was observed. The third and fourth steps are slow with activation energies of 16.59 and 23.51 kJ mol⁻¹, respectively and the order of reactions are observed to be of first order for both the steps. The final residue, estimated as zinc oxide.

Non-isothermal calculations were used extensively to evaluate kinetic parameters for the different thermal decomposition steps in the complexes employing the Horowitz–Metzger equations [39]. The results of activation enthalpy ($\Delta H^\# = E_a - RT_s$); the activation entropy ($\Delta S^\# = 2.303[\log Ah/RT]R$); the pre-exponential factor ($E_a/R T_s^2 = A/\Phi \exp[-E_a/RT_s]$) and the free energy of activation ($\Delta G^\# = \Delta H^\# - T_s \Delta S^\#$) are given in Table 5, where A , Φ , T_s , K and h are the pre-exponential factor, heating rate, peak temperature,

Boltzman and Plank constants, respectively [40]. The negative $\Delta S^\#$ values for all decomposition steps in the complexes indicate that the complexes are more ordered [41]. The kinetic parameters, especially energy of activation (E_a) is helpful in assigning the strength of the bonding of ligand moieties with the metal ion. The calculated E_a values of the investigated heterochelates for the degradation stage of ligand (benen) are in the range 13.64–20.54 kJ mol⁻¹. The relative high E_a value indicates that the ligand (benen) is strongly bonded to the metal ion [15]. From the above discussion an octahedral structure of the heterochelates can tentatively be assumed as shown in Figs 5 and 6.



where M=Mn(II), Co(II) and Cu(II), n=0;
M=Zn(II), n=0.5; M=Ni(II), n=1

Fig. 5 The suggested structure of heterochelates

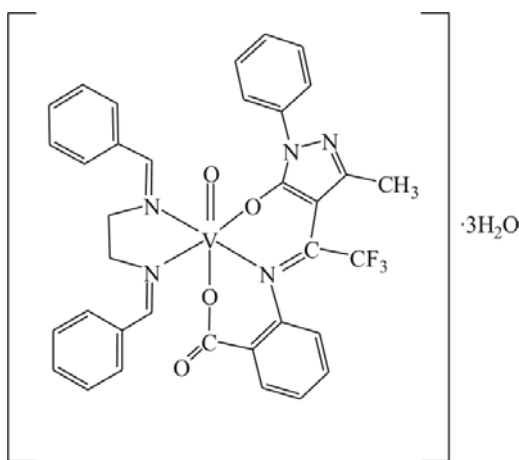


Fig. 6 The suggested structure of $[\text{VO}(\text{SB})(\text{benen})]\cdot 3\text{H}_2\text{O}$

Acknowledgements

We wish to express our gratitude to the Head, Department of Chemistry, Sardar Patel University, Vallabh Vidyanagar, Gujarat, India for providing the necessary laboratory facilities.

References

- 1 A. A. Soliman, *J. Therm. Anal. Cal.*, 63 (2001) 221.
- 2 G. G. Mohamed, F. A. Nour El-Dien and Nadia E. A. El-Gamel, *J. Therm. Anal. Cal.*, 67 (2002) 135.
- 3 G. G. Mohamed and Z. H. Abd El-Wahab, *J. Therm. Anal. Cal.*, 73 (2003) 347.
- 4 H. A. El-Boraey, *J. Therm. Anal. Cal.*, 81 (2005) 339.
- 5 C. L. Albano, R. Sciamanna, T. Aquino and J. J. Martinez, European Congress on Computational Methods in Applied Sciences and Engineering, ECOMAS 2000, Barcelona, 11–14 September, 2000.
- 6 F. Carrasco, *Thermochim. Acta*, 213 (1993) 115.
- 7 S. H. Patel, P. B. Pansuriya, M. R. Chhasatia, H. M. Parekh and M. N. Patel, *J. Therm. Anal. Cal.*, 91 (2008) 413.
- 8 A. I. Vogel, *Textbook of Practical Organic Chemistry*, 5th Edn. Longman, London 1989.
- 9 E. C. Okafor, *Talanta*, 29 (1982) 275.
- 10 A. C. Effendy, F. Marchetti, C. Pettinari, R. Pettinari, B. W. Skelton and A. H. White, *Inorg. Chem.*, 43 (2004) 4387.
- 11 P. P. Dholakiya and M. N. Patel, *Synth. React. Inorg. Met.-Org. Chem.*, 32 (2002) 819.
- 12 A. I. Vogel, *A Textbook of Quantitative Inorganic Analysis*, 3rd Edn. Longman, London 1975, pp. 433.
- 13 N. H. Furman, *Standard Methods of Chemical Analysis*, Vol. I, 6th Edn., D. Van Nostrand Company, Inc., New Jersey 1962, pp. 1211.
- 14 P. K. Panchal and M. N. Patel, *Synth. React. Inorg. Met.-Org. Chem.*, 34 (2004) 1277.
- 15 H. M. Parekh, P. K. Panchal and M. N. Patel, *J. Therm. Anal. Cal.*, 86 (2006) 803.
- 16 P. K. Panchal, H. M. Parekh and M. N. Patel, *Toxicol. Environ. Chem.*, 87 (2005) 313.
- 17 B. S. Creaven, D. A. Egan, K. Kavanagh, M. McCann, A. Noble, B. Thati and M. Walsh, *Inorg. Chim. Acta*, 359 (2006) 3976.
- 18 P. B. Pansuriya and M. N. Patel, *J. Enz. Inhib. Med. Chem.*, 23 (2008) 108.
- 19 C. K. Modi and B. T. Thaker, *Indian J. Chem.*, 41A (2002) 2544.
- 20 L. Liu, D. Jia and Y. Ji, *Synth. React. Inorg. Met.-Org. Chem.*, 32 (2002) 739.
- 21 M. Mohapatra, V. Chakravortty and K. C. Das, *Polyhedron*, 8 (1989) 1509.
- 22 H. Köksal, M. Tûmer and S. Serin, *Synth. React. Inorg. Met.-Org. Chem.*, 26 (1996) 1577.
- 23 A. B. P. Lever, *Inorganic Electronic Spectroscopy*, 2nd Edn. Elsevier, Amsterdam 1984.
- 24 M. Sönmez, *Polish J. Chem.*, 77 (2003) 397.
- 25 R. Carbello, A. Cartineiras, W. Hiller and J. Strahle, *Polyhedron*, 13 (1993) 1083.
- 26 A. A. Osowole, J. A. O. Woods and O. A. Odunola, *Synth. React. Inorg. Met.-Org. Chem.*, 32 (2002) 783.
- 27 M. Kwiatkowski, A. Kwiatkowski, A. Olechnowicz, D. M. Ho and E. A. Deutsch, *J. Chem. Soc. Dalton Trans.*, (1990) 2497.
- 28 O. Z. Yeşilel, H. İçbudak, H. Ölmez and Panče Naumov, *Synth. React. Inorg. Met.-Org. Chem.*, 33 (2003) 77.
- 29 A. L. Abuhiyleh, C. Woods and I. Y. Ahmed, *Inorg. Chim. Acta*, 190 (1991) 1.
- 30 H. M. Parekh, P. B. Pansuriya and M. N. Patel, *Pol. J. Chem.*, 79 (2005) 1843.
- 31 E. König, *Structure and Bonding*, Springer Verlag, New York 1971, pp. 9, 175.
- 32 E. S. Freeman and B. Carroll, *J. Phys. Chem.*, 62 (1958) 394.
- 33 C. K. Modi, S. H. Patel and M. N. Patel, *J. Therm. Anal. Cal.*, 87 (2007) 441.
- 34 G. G. Mohamed and Z. H. Abd El-Wahab, *J. Therm. Anal. Cal.*, 73 (2003) 347.
- 35 G. G. Mohamed, F. A. Nour El-Dien and Nadia E. A. El-Gamel, *J. Therm. Anal. Cal.*, 67 (2002) 135.
- 36 S. B. Jagtap, R. C. Chikate, O. S. Yemul, R. S. Ghadage and B. A. Kulkarni, *J. Therm. Anal. Cal.*, 78 (2004) 251.
- 37 P. B. Pansuriya, P. Dhandhukia, V. Thakkar and M. N. Patel, *J. Enz. Inhib. Med. Chem.*, 22 (2007) 477.
- 38 N. M. El-Metwally, I. M. Gabr, A. M. Shallaby and A. A. El-Asmy, *J. Coord. Chem.*, 58 (2005) 1145.
- 39 H. H. Horowitz and G. Metzger, *Anal. Chem.*, 25 (1963) 1464.
- 40 R. M. Mahfouz, M. A. Monshi, S. M. Alshehri, N. A. El-Salam and A. M. A. Zaid, *Synth. React. Inorg. Met.-Org. Chem.*, 31 (2001) 1873.
- 41 A. A. Aly, A. S. A. Zidan and A. I. El-Said, *J. Thermal Anal.*, 37 (1991) 627.

Received: November 26, 2007

Accepted: January 22, 2008

OnlineFirst: August 15, 2008

DOI: 10.1007/s10973-007-8790-4